

Parametric Investigation of Store Separation Including Unsteady Effects

Kevin Roughen^{*}, Steven Doyle[†]
M4 Engineering, Inc., Long Beach, CA, 90807

Rajan Kumar[‡], Greg Robertson[§]
Florida A&M University and Florida State University, Tallahassee, FL, 32310

Ian Maatz^{**}, Rudy Johnson^{††}
Air Force Research Lab, Aerospace Systems Directorate, WPAFB, OH, 45433

Parametric investigation has been performed including unsteady effects. In a first method, variation in mass properties and flight conditions are investigated. Trajectory simulations are conducted including unsteady effects and surrogate models are constructed based on their results. In a second method, intermediate data such as unsteady grid loads are formulated based on the results of lower fidelity analyses. In both cases, parametric studies are performed establishing relationships between store parameters and the occurrence of trajectory variations.

I. Introduction

Accurate prediction of the trajectory of a store upon separation from an aircraft is vital to safe operation. Steady state methods have been developed for progressing along a separation trajectory using aerodynamic data relevant at each state along that trajectory [1]. While this is adequate for many configurations, reduction in mass and stability can create stores that are susceptible to unsteady flows, such as those found in weapons bays. These cases cannot be accurately predicted with steady methods, and require collection of time-accurate unsteady data [2], [3].

Inclusion of unsteady aerodynamic effects presents computational challenges. One method involves the use of time accurate Computational Fluid Dynamic (CFD) analysis coupled with 6-DOF simulation [4], [5]. The time accurate CFD analyses used in this approach require significant computational resources. A separate time accurate CFD analysis must be performed for each release event simulated. An alternative approximate engineering method is to generate a database of unsteady aerodynamic grid loads for use in a trajectory modeling code [3]. While this approach can be run rapidly to simulate many release times once unsteady grid data is present, the computational expense associated with the CFD runs to create the unsteady database is still significant. This approach is used in the current work to provide training data for surrogate modeling methods. Obtaining unsteady grid loads through wind tunnel testing is possible but the technology required for this has yet to be widely adopted.

Surrogate modeling presents an opportunity to efficiently characterize a broad parameter space. In general, this concerns the development of a mathematical model which learns the input output relationship for a given system from training data. This model can then be applied to predict output for new parametric inputs. A broad range of surrogate modeling methods have been developed. The current work makes use of the Non-Intrusive Polynomial Chaos [6], Naïve Bayes [7], and Artificial Neural Network [7] methods.

^{*} Vice President of Engineering, Member, AIAA.

[†] Senior Engineer, Member, AIAA.

[‡] Associate Professor, Department of Mechanical Engineering, Associate Fellow AIAA.

[§] Graduate Research Assistant, Department of Mechanical Engineering, Student Member AIAA.

^{**} Aerospace Engineer, Integrated Systems Branch, AFRL/RQVI.

^{††} Weapons Integration Team Lead, AFRL/RQVI.

In the present work, parametric variations and surrogate modeling techniques are applied to simulate a broad range of store configurations. Observations are made about the relationships between store parameters and trajectory deviations.

II. Technical Approach

A. Configurations for High Fidelity Simulation and Experiment

Data from two separate wind tunnel tests are used as baseline demonstration problems. The first is a set of drop test described in reference [3] that simply tried to obtain repeatable separation trajectories at the Mach 0.8 test conditions. The second data set looks at geometry variation of the store model while keeping the weapons bay geometry fixed. This data set was generated by M4 Engineering and the FCAAP center at FSU and has not been previously published.

1. Parametrically Modified HIFEX/GBU-38

Parametric investigation was performed by varying mass property, release conditions, and flight condition data for the HIFEX/GBU-38 configuration described in Ref. [3] (Figure 1). Eight input parameters were randomly sampled from Gaussian distributions as described in Table 1. The resulting configurations were filtered to remove non-physical cases. Steady and unsteady aerodynamic grid data were calculated using time-accurate CFD analysis at a single flight condition. As such, the effect of altitude on dynamic pressure is captured, but the effect on Reynolds number is not. Note that mass and moment of inertia were varied independently which can lead to creation of stores with unlikely mass distributions. Over four thousand configurations were generated and analyzed with the FLIP-RUSAT process (discussed in the next section).

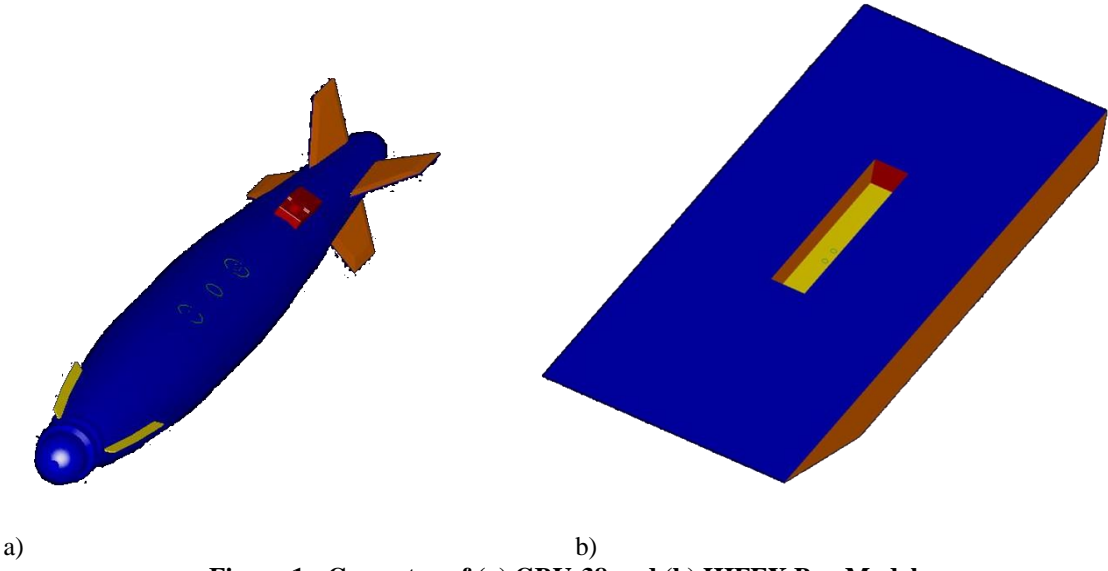


Figure 1: Geometry of (a) GBU-38 and (b) HIFEX Bay Model.

Table 1: Input Parameters (x) with Mean & Standard Deviation.

| Input (x) Parameter | FLIP4 Parameter | Mean | Standard Deviation |
|------------------------------|--------------------|---------------------------|-----------------------|
| Altitude, h | ALT | 15000 | 7500 ft |
| Reference Area, S_{ref} | SREF | 0.9076 in ² | 0.500 in ² |
| Reference Length, chord, c | LREF_PITCH | 1.075 in | 0.5 in |
| CG Location, x_{CG} | XCG | 5.666 in ² | 2.666 in ² |
| Mass, m | MASS | 234.78 g | 100 g |
| Pitching Inertia, I_{yy} | IYY | 1086.14 g/in ² | 500 g/in ² |
| Initial Z Velocity, w_0 | INITIAL_COND[:,6] | -150 in/s | 100 in/s |
| Initial Pitch Rate, q_0 | INITIAL_COND[:,11] | 0.0 rad/s | 5.0 rad/s |

2. L/D 4.5 Cavity with Generic Store Models

A generic store model was designed for testing in the polysonic wind tunnel at FSU. A wall mounted L/D 4.5 cavity model was used to simulate the weapons bay at a freestream Mach number of 2.0. In order to investigate the effects of variation in length and fin size, four generic geometries were created. These stores are referred to based on the length of the store and the size of the fins. For instance, the Short Store Small Fin configuration is referred to as SSSF. Selected parameters for these stores are shown in Table 2 as wind tunnel model scale and at full scale. A photo of the SSSF wind tunnel model is shown in Figure 2.

Table 2: Parameter Values for Selected Configurations

| | | SSSF (model scale) | SSLF (model scale) | LSSF (model scale) | LSLF (model scale) | SSSF (full scale) | SSLF (full scale) | LSSF (full scale) | LSLF (full scale) |
|-------------|-------------------|--------------------|--------------------|--------------------|--------------------|-------------------|-------------------|-------------------|-------------------|
| Aerodynamic | Length | (in) | 6.4 | 6.4 | 8.0 | 8.0 | 64 | 64 | 80 |
| | Diameter | (in) | 0.80 | 0.80 | 0.80 | 0.80 | 8.0 | 8.0 | 8.0 |
| | Wingspan | (in) | 1.6 | 2.4 | 1.6 | 2.4 | 16 | 24 | 16 |
| | Span / Diameter | | 2.0 | 3.0 | 2.0 | 3.0 | 2.0 | 3.0 | 3.0 |
| | Slenderness ratio | | 8.0 | 8.0 | 10.0 | 10.0 | 8.0 | 8.0 | 10.0 |
| Inertial | Mass | (lb) | 0.25 | 0.25 | 0.30 | 0.30 | 250 | 250 | 300 |
| | Pitch Inertia | (slug-ft^2) | 1.3E-04 | 1.3E-04 | 2.5E-04 | 2.5E-04 | 13.4 | 13.4 | 25.1 |
| | Roll Inertia | (slug-ft^2) | 4.0E-06 | 4.0E-06 | 4.8E-06 | 4.8E-06 | 0.40 | 0.40 | 0.48 |
| | CG Station | (x/L) | 0.49 | 0.49 | 0.49 | 0.49 | 0.49 | 0.49 | 0.49 |
| | CG Station | (in) | 3.11 | 3.11 | 3.89 | 3.89 | 31.1 | 31.1 | 38.9 |



Figure 2: Wind Tunnel Model of SSSF Configuration [8]

B. Simulation Methods

1. High-Fidelity Approach (FLIP-RUSAT)

FLIP is the standard AFSEO store separation trajectory analysis code that has been supplemented with the Rapid Unsteady Store Analysis Tool (RUSAT) as described in Ref. [3] and illustrated in Figure 3. This approach simulates an ensemble of trajectories resulting from drops with varied release time. This approach requires aerodynamic data from Computational Fluid Dynamics (CFD) analysis or wind tunnel testing to create databases of steady aerodynamic force and moment as a function of attitude and position. Unsteady aerodynamic force and moment power spectral density (PSD) data as a function of position and frequency is also obtained from the time accurate CFD. This analysis process is shown in Figure 4. While this process is relatively straightforward, it requires steady and unsteady grid data which is computationally expensive to obtain.

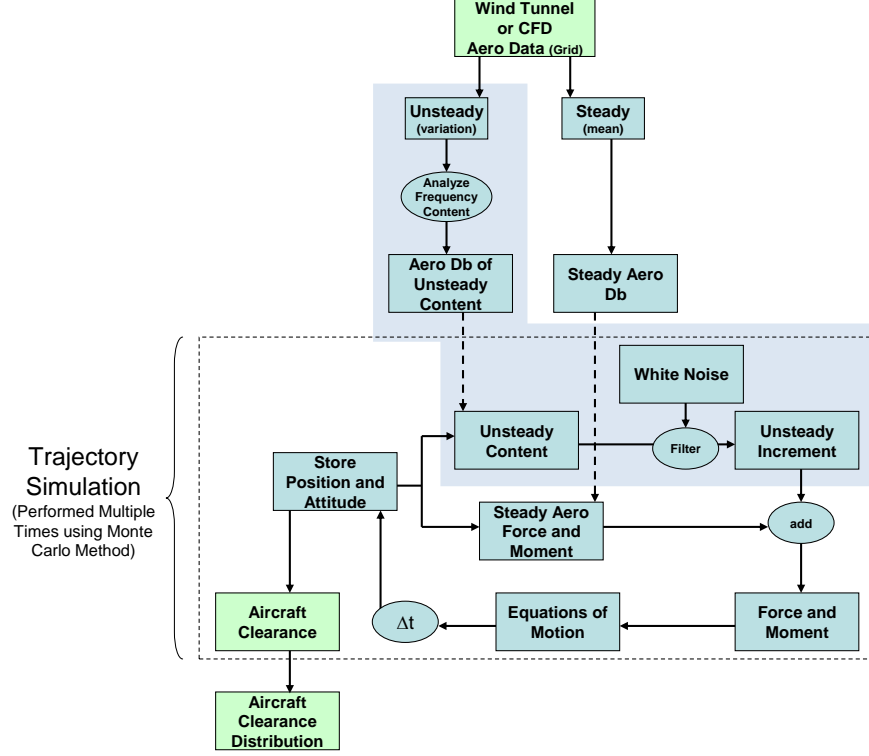


Figure 3: Store Separation Analysis with Unsteady Effects.

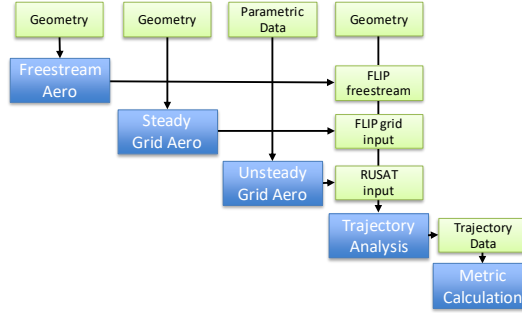


Figure 4: High Fidelity Process

In Ref. [3] the FLIP-RUSAT approach demonstrated the capability to model the GBU-38 separation trajectories from the modified HIFEX weapons bay model. New FLIP-RUSAT trajectory simulations are compared to wind tunnel drop test data for the SSLF and LSLF configurations (Figure 5 and Figure 6). The stores are separated from a L/D 4.5 cavity with a freestream Mach number of 2.0. Simulations are performed using steady aerodynamic loads from wind tunnel testing and an unsteady aerodynamic database from CFD analysis. Reasonable correlation in position is observed for both stores. The SSLF configuration exhibits good correlation in the amplitude and frequency of pitch angle oscillation. The variation in the wind tunnel trajectories is large relative to the predicted standard deviation from FLIP-RUSAT. This could indicate higher than predicted unsteady loads in the wind tunnel. Significant differences are noted in the pitch angle results from simulation and drop test for the LSLF. In particular, the wind tunnel trajectories exhibit higher amplitude and larger variation in pitch angle oscillation. A number of factors including variation in the initial release conditions during wind tunnel test could cause this behavior.

SSLF Configuration Trajectory Results (Stochastic)

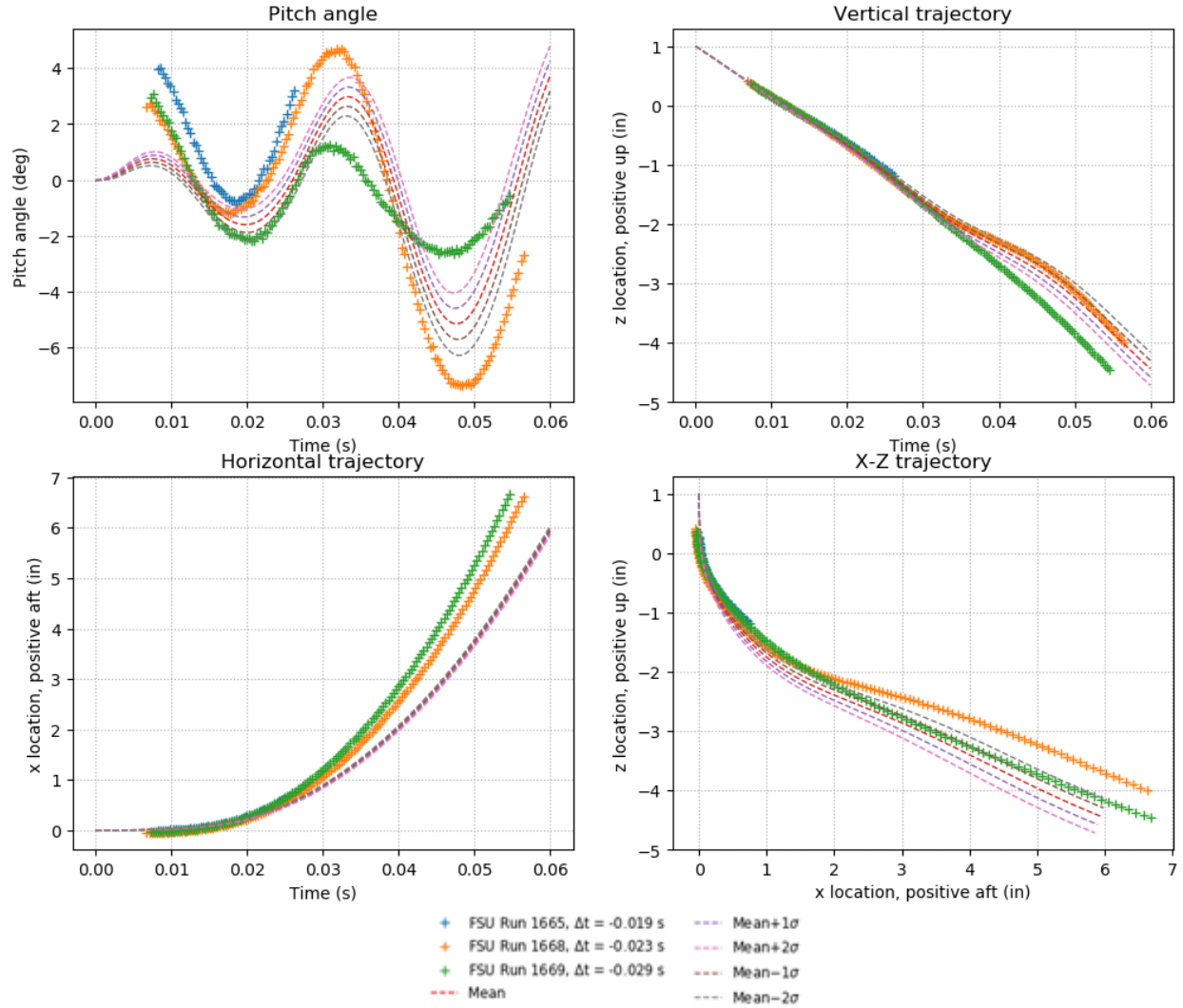


Figure 5: Stochastic trajectory results for the SSLF configuration.

LSLF Configuration Trajectory Results (Stochastic)

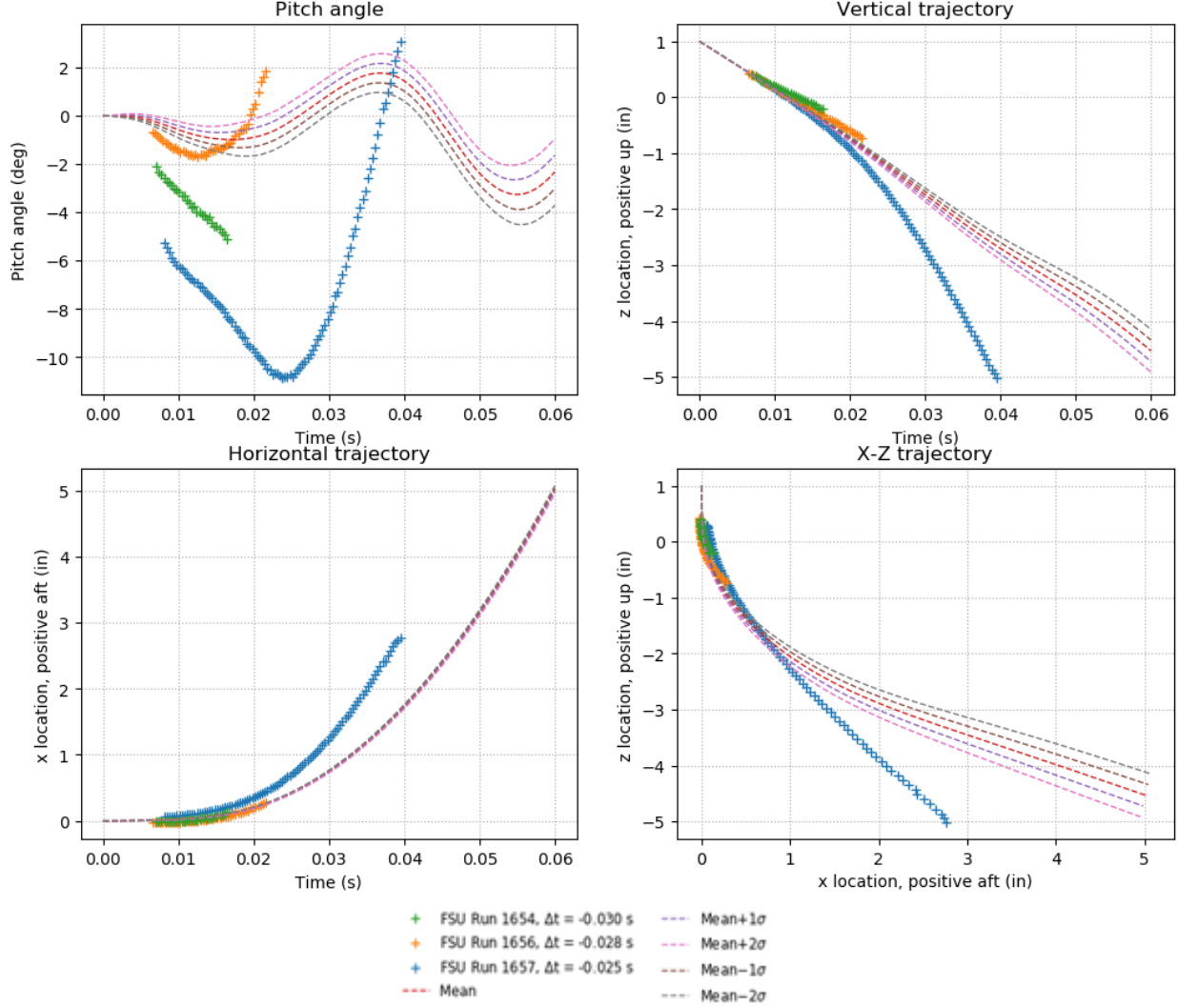


Figure 6: Stochastic trajectory results for the LSLF configuration.

2. Rapid Parametric Process

Due to the computational expense associated with building a high-fidelity simulation database, a low fidelity capability has been developed. This low fidelity capability computes “input metrics” (e.g. ratio of Rossiter to freestream short period frequencies) using only a simple set of input parameters (e.g. mass, length, ...). This process parametrically modifies a Datcom model to compute stability derivatives used in a flight dynamics calculation (Figure 7). Simple models of unsteady aerodynamic data are included in the form of low-order frequency response functions parameterized by Rossiter frequency, amplitude, and damping. Note that modules of this process can be run to investigate how the physical phenomena affecting trajectories interact.

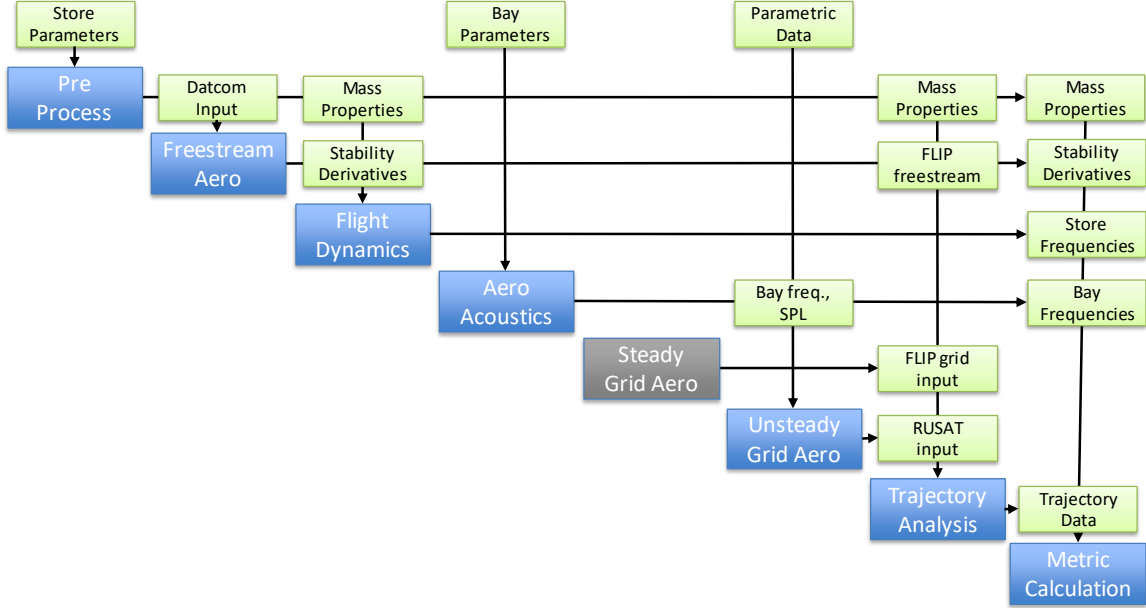


Figure 7: Rapid-Parametric Process

C. Surrogate Modeling

Surrogate models are constructed to represent the relationship between characteristics of the store, bay, and ejector and the resulting trajectory. Once generated, these models can be evaluated rapidly for a wide range of parameter variations. Three alternate formulations are discussed and results for the first two are presented. These models are trained using a database generated by the FLIP-RUSAT model.

1. Orthogonal Polynomial

An orthogonal polynomial approach is used based on point collocation Non-Intrusive Polynomial Chaos (NIPC) method described in Refs. [6], [9], [10], and [11]. In this approach, a linear system of equations:

$$\begin{bmatrix} \Psi_0(\vec{\xi}_0) & \Psi_1(\vec{\xi}_0) & \dots & \Psi_P(\vec{\xi}_0) \\ \Psi_0(\vec{\xi}_1) & \Psi_1(\vec{\xi}_1) & \dots & \Psi_P(\vec{\xi}_1) \\ \vdots & \vdots & \ddots & \vdots \\ \Psi_0(\vec{\xi}_P) & \Psi_1(\vec{\xi}_P) & \dots & \Psi_P(\vec{\xi}_P) \end{bmatrix} \begin{Bmatrix} \alpha_0(\vec{x}, t) \\ \alpha_1(\vec{x}, t) \\ \vdots \\ \alpha_P(\vec{x}, t) \end{Bmatrix} = \begin{Bmatrix} \alpha^*(\vec{x}, t, \vec{\xi}_0) \\ \alpha^*(\vec{x}, t, \vec{\xi}_1) \\ \vdots \\ \alpha^*(\vec{x}, t, \vec{\xi}_P) \end{Bmatrix} \quad (1)$$

is developed in which uncertain response variables α^* are expressed in terms of a deterministic component α_j and basis functions Ψ_j . These quantities are functions of an input variable vector \vec{x} and a random variable vector $\vec{\xi}$. A Least Squares solution is performed to solve for the deterministic component and provide an estimate for output in terms of input.

2. Naïve Bayes

Bayesian models [7] define input output relationships based on a network of conditional probabilities. A simple network is considered in which the trajectory characteristics (output metrics) are dependent on the parameters of the configuration (input metrics). In this simple model, the inputs are considered to be independent of each other. This assumption of independence among the inputs allows the use of a Naïve Bayes model in which the output estimate can be determined using the expression:

$$P(y | x_1, \dots, x_n) = \frac{P(y) \prod_{i=1}^n P(x_i | y)}{P(x_1, \dots, x_n)} \quad (2)$$

where the probabilities $P(y)$, $P(x_i | y)$, and $P(x_1, \dots, x_n)$ can be learned from training data. In the current work, these probability distributions are assumed to be Gaussian.

3. Artificial Neural Networks (ANN)

In the case of ANNs, the process for computing output from a vector of inputs is done using a network of units, connected by links [7] (Figure 8). Each unit propagates the activation a_i to a_j using a weight $w_{i,j}$ and an activation function g :

$$a_j = g\left(\sum_{i=0}^n w_{i,j} a_i\right) \quad (3)$$

In order to facilitate numerical differentiation, a sigmoid function can be used for $g()$:

$$g(\alpha) = \frac{1}{1 + e^{-\alpha}} \quad (4)$$

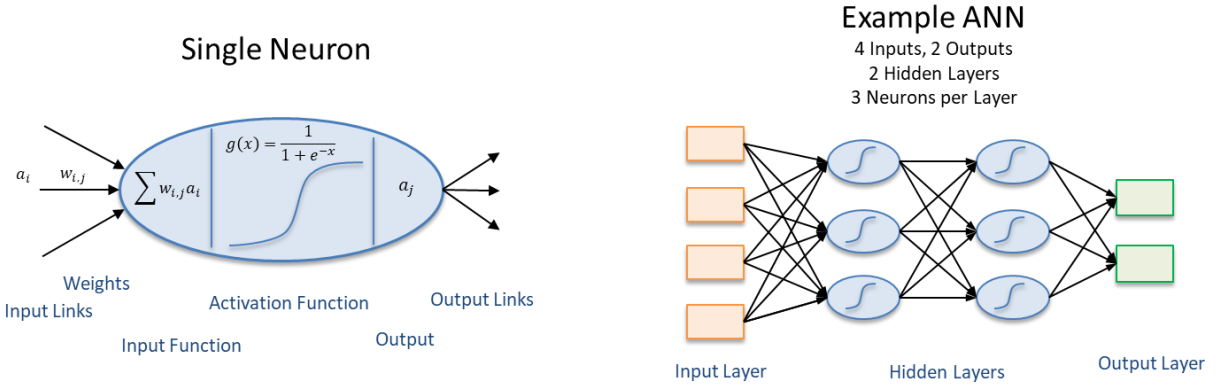


Figure 8 Illustration of ANN with Two Hidden Layers.

Once this is done, training can be performed by updating the weights in the network to minimize the difference between the output of the network and the known output in the training set. A process known as backpropagation is used to compute partial derivatives of this error with respect to the weights. These derivatives can then be used in a gradient based optimization process to develop a set of weights that comprise a trained network that can be used to map new inputs to unknown outputs.

III. Results of Parametric Simulations

A. Effect of Mass Properties on Store Trajectory

Mass property variation was investigated for a HIFEX/GBU-38 configuration at Mach 0.8 freestream conditions. A detailed description of the baseline configuration as well as the simulation methodology is presented in Ref. [3]. Maximum angle of attack (α_{\max}) was chosen as a quantitative output metric considered to be associated with undesirable trajectory deviations. Surrogate models were developed for the maximum angle of attack across the trajectory for 4441 samples with variation in input parameters (Table 1), in addition to variation due to unsteady aerodynamic loads. The validity of these models was then investigated using an independent cross validation set of 1,000 additional samples generated using the FLIP-RUSAT model.

It is possible to observe correlations between input variables and the maximum angle of attack. In Figure 9 the 1,000 cross-validation datapoints are plotted in red while the surrogate model results are plotted in blue. The maximum angle of attack increases as the center of gravity moves aft. This trend coincides with intuition due to the fact that cases with aft CG will have decreased static stability margin. Another trend that can be observed is that maximum angle of attack decreases for cases with increased initial velocity (Figure 10). This is consistent with a consideration that cases with higher initial velocity will spend less time in the shear layer and are less likely to undergo a pitch deviation due to the forces encountered there. Observation of the validation data and the orthogonal polynomial (NIPC) and Naïve Bayes models shows that the trends in the validation data are present in both surrogate methods. Additionally, it can be observed that there is significant scatter relative to the trend in all three

datasets. This scatter is due to both the influence of other parameters, as well as variability due to the unsteady aerodynamic environment.

The effectiveness of the models in fitting the data is quantified by dividing the root mean square discrepancy of the output by the average value of the output. These differences between the models and the cross-validation data are shown in Table 3. All three surrogate model forms predict the value of the maximum angle of attack within 14%. In fact, the orthogonal polynomial based method predicts the maximum angle of attack within 9%.

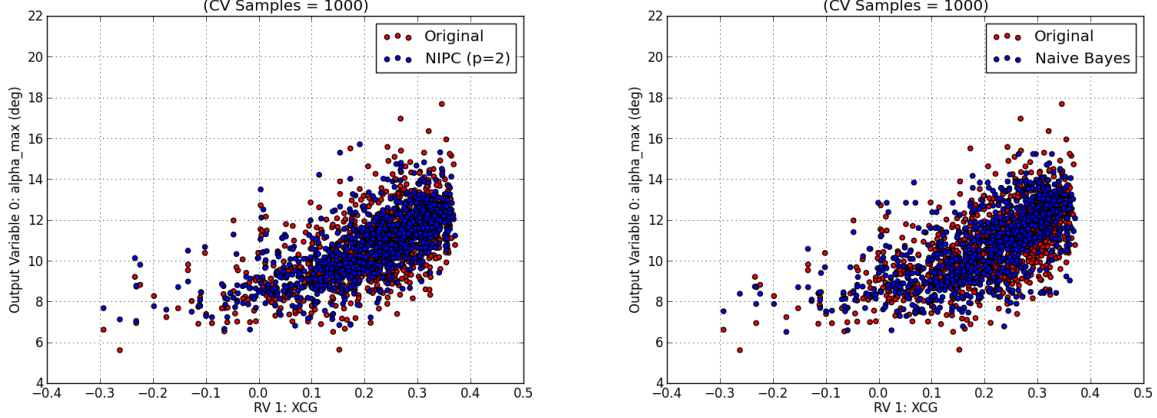


Figure 9: Plot of Maximum Angle of Attack vs. Axial Center of Gravity Location.

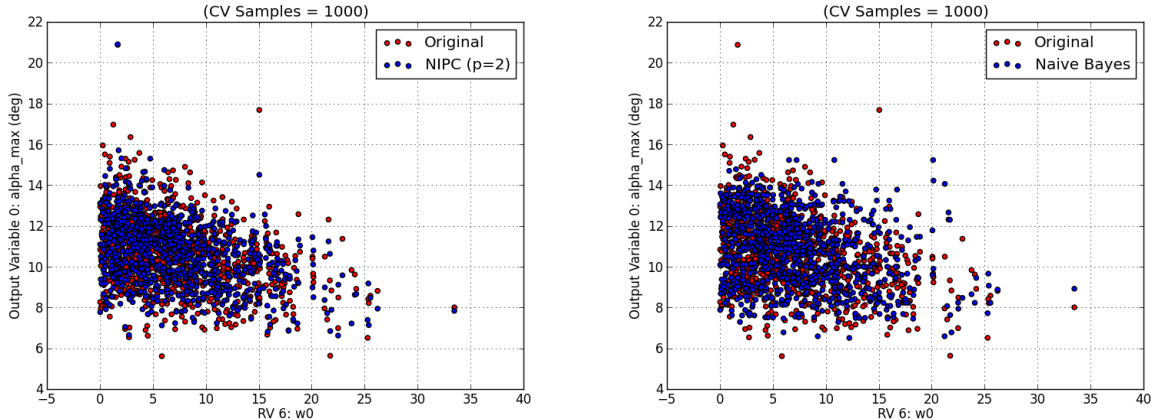


Figure 10: Plot of Maximum Angle of Attack vs. Initial Velocity.

Table 3: Comparison of Discrepancy between Mean Model Prediction and Sample Data for Maximum Angle of Attack (α_{\max}) based on 1,000 Validation Samples.

| Training Method (4,441 Samples) | Cross Validation (1,000 Samples) | Rank |
|---|----------------------------------|------|
| Orthogonal Polynomial (2 nd order) | 8.35% | 1 |
| Artificial Neural Network | 10.20% | 2 |
| Naïve Bayes | 13.82% | 3 |

B. Effect of Store and Bay Parameters on Flight Dynamic and Aeroacoustic Frequencies

The Freestream Aerodynamics, Flight Dynamics, and Aeroacoustics modules from the Rapid Parametric Process described in Figure 7 above were performed on the baseline LSLF store model at full scale. Flight dynamics calculations on this vehicle show a prominent short period peak at 2.4Hz (Figure 11). The transmissibility of the

vehicle system decreases greatly above 4Hz. While this is a simple approximation based on the freestream aerodynamics, it suggests that bay frequency content above 4Hz is less likely to excite trajectory deviations. Calculation of the bay frequencies using the Rossiter equation indicates a first mode frequency at 62 Hz (Figure 12). A trade study is performed in which the size of the store is reduced maintaining the mass density. Various store geometries are considered by varying slenderness ratio and fin span ratio as shown in Table 4. The short period frequency is calculated for this variation in weight for stores with several fin sizes. Additionally, the Rossiter frequencies are calculated for bays of various sizes.

Results for store short period frequency, and cavity Rossiter frequency for a range of stores and cavities is shown in Figure 13. The results suggest that the cavity and flight dynamic frequencies are more likely to interact for the case of stores weighing less than 30lb. In particular, a 32" long store with slenderness ratio of 10 and fin span ratio of 5 has a short period frequency that is the same as the first Rossiter frequency for a 360" long bay. The time taken to transit the shear layer excluding aerodynamic forces for a gravity drop is also calculated. This is plotted in Figure 13 and suggests that this may interact with flight dynamics for a 150lb store.

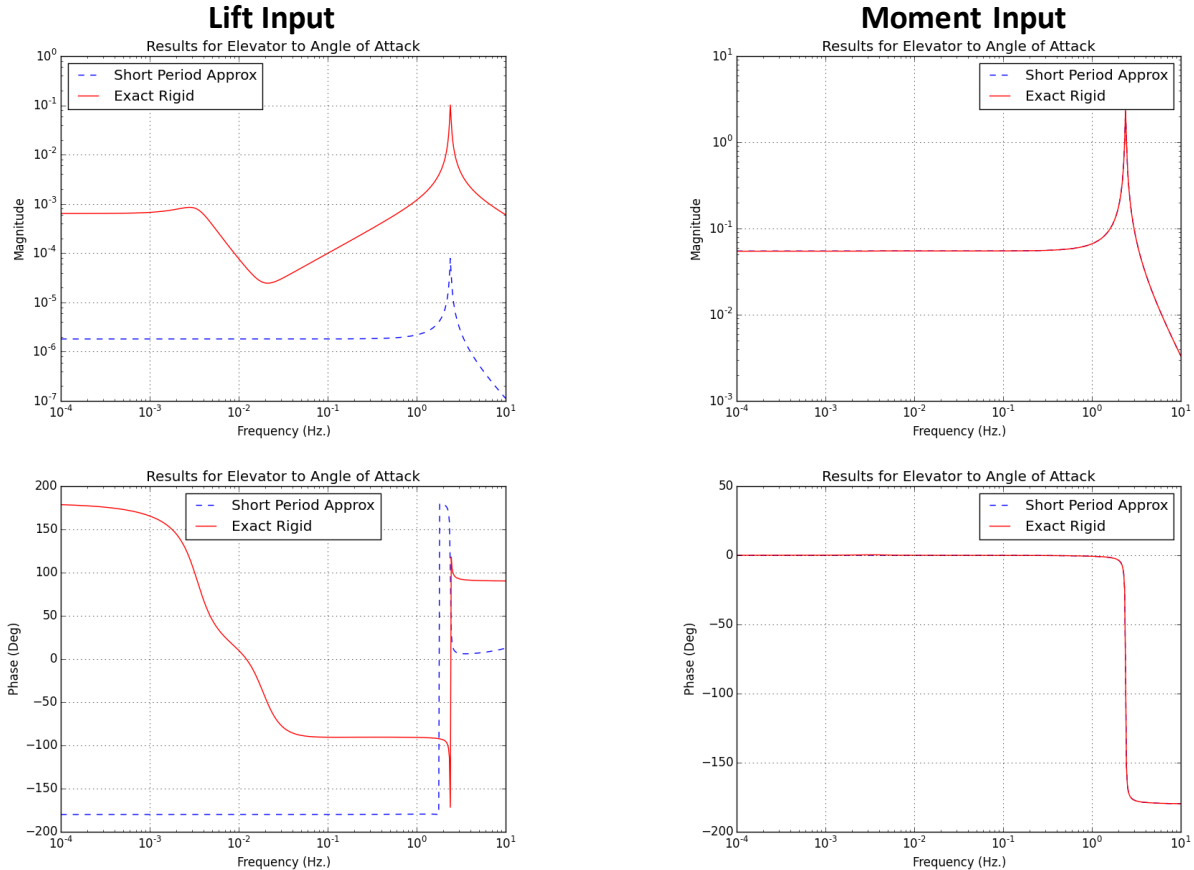
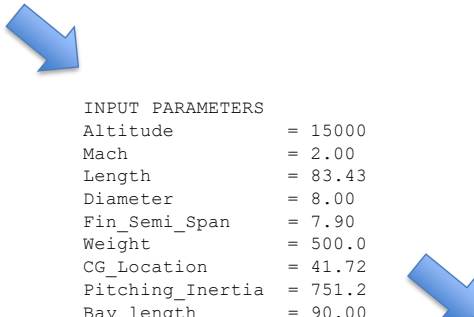


Figure 11: Pitch Loop Results (500lb LSLF Example)

```

ulst2inputs = {
    'g': 386.087, # in / s^2
    # bay
    'bay_length' : 90., # in
    'bay_depth' : 20., # in
    'Kv_bay' : 0.57,
    # store
    'diameter' : 8., # in
    'length': 83.43, # in
    'semi_span': 7.9, # in
    'x_cg': 0.5, # percent
    'weight': 500., # pounds
    'Jxp': 41.441
    'Jyp': 751.185
    # FC
    'uinf': 25357.64, # in/sec
    'alt': 15000.,
}

```



| INPUT PARAMETERS | |
|------------------|---------|
| Altitude | = 15000 |
| Mach | = 2.00 |
| Length | = 83.43 |
| Diameter | = 8.00 |
| Fin_Semi_Span | = 7.90 |
| Weight | = 500.0 |
| CG_Location | = 41.72 |
| Pitching_Inertia | = 751.2 |
| Bay_length | = 90.00 |
| Bay_depth | = 20.00 |

| INPUT METRICS | |
|-------------------|---------|
| First_bay_freq | = 62.3 |
| Short_period_freq | = 27.4 |
| Frequeny_ratio | = 26.00 |
| Dynamic_pressure | = 23.21 |
| Static_margin | = 1.94 |
| Weight_over_drag | = 0.87 |
| Wght_ov_lift_5deg | = 0.52 |

Figure 12: Configuration shows large spacing between cavity and short period frequency.

Table 4: Store Parameters Considered.

| Store Identification | Slenderness Ratio | Fin Span Ratio | Weight to Volume Ratio |
|----------------------|-------------------|----------------|------------------------|
| 1 | 10 | 3.0 | 0.119 |
| 2 | 10 | 4.0 | 0.119 |
| 3 | 10 | 5.0 | 0.119 |
| 4 | 15 | 3.8 | 0.119 |

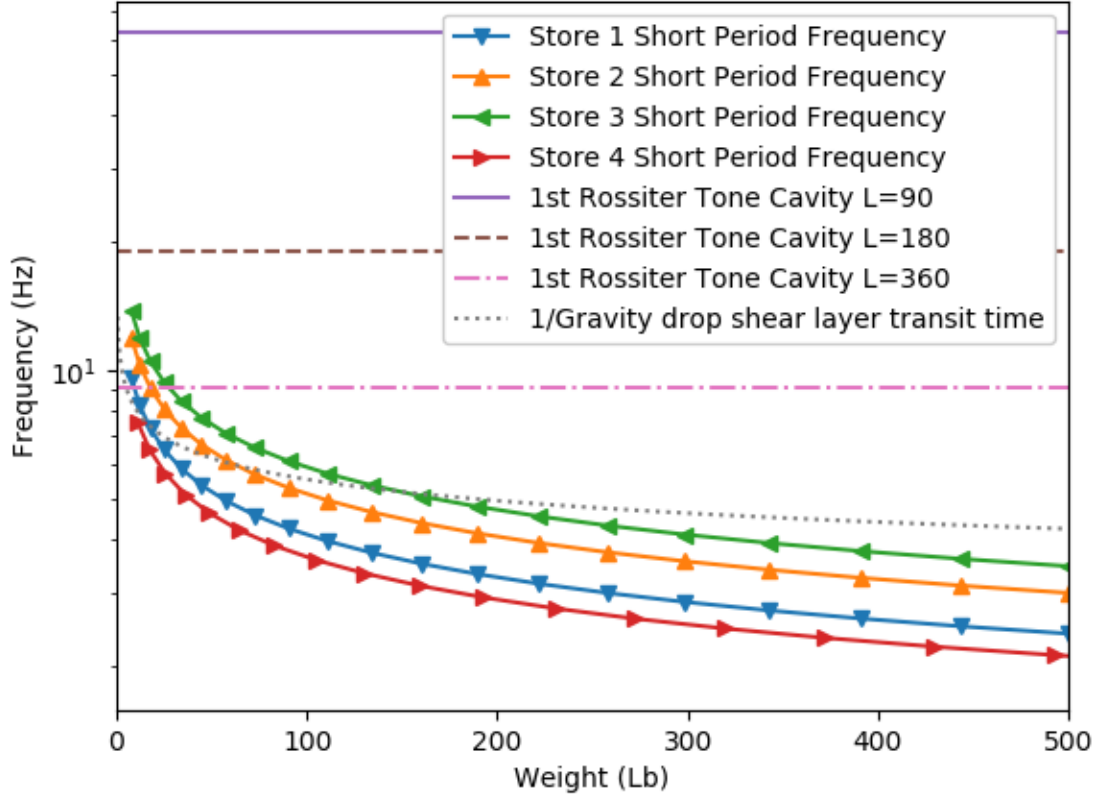


Figure 13: Short period and Rossiter frequencies coincide for the case of small store in large bay.

C. Effect of Aeroacoustic Frequency on Trajectory

A low fidelity parametric unsteady load variation study was conducted for the SSLF scale model configuration using FLIP-RUSAT. Steady aerodynamic data was taken from wind tunnel test and unsteady aerodynamic loading was represented with simple parametric frequency domain representations with the peak frequency considered as an input parameter (Figure 14). The unsteady loading is considered to act in a region near the shear layer by varying the magnitude of the loading as shown in Figure 15. Aside from the aerodynamic frequency of the unsteady content, the store properties and other inputs remain unchanged. For this configuration under the conditions prescribed, the store would exit the region of unsteady loading at 0.025 seconds after release when aerodynamic forces are neglected. The frequency of the pitching motion of the baseline configuration was found to be 33 Hz or at a period of 0.03 seconds. FLIP-RUSAT simulations are performed while varying the frequency of aeroacoustic loading. Fifty realizations are considered for each frequency considering the effect of varying release time. Statistics are computed from each ensemble of trajectories to calculate the mean and standard deviation of pitch angle and z-location at each time. These statistics are combined to create trajectories corresponding to mean, mean minus two sigma (standard deviation), and mean plus two sigma. These trajectories are post processed to calculate the maximum pitch angle and the ratio of the actual z location 0.075 seconds after release to the z location that would result from a ballistic trajectory (z-ratio). Varying the aeroacoustic frequencies between 0 to 800 Hz, the maximum pitch angle of the mean plus two sigma trajectory and z-ratio from the mean minus two sigma trajectory can be seen in Figure 16. Note that trajectory deviations correspond to large maximum pitch angles and small z-ratios. There is an increase in trajectory deviations for the case with aerodynamic modes at 75 and 150 Hz. There is also an overall increase in deviations at lower frequencies. Stochastic trajectories under unsteady aerodynamics with modes at 75 Hz and 800 Hz can be seen in Figure 17.

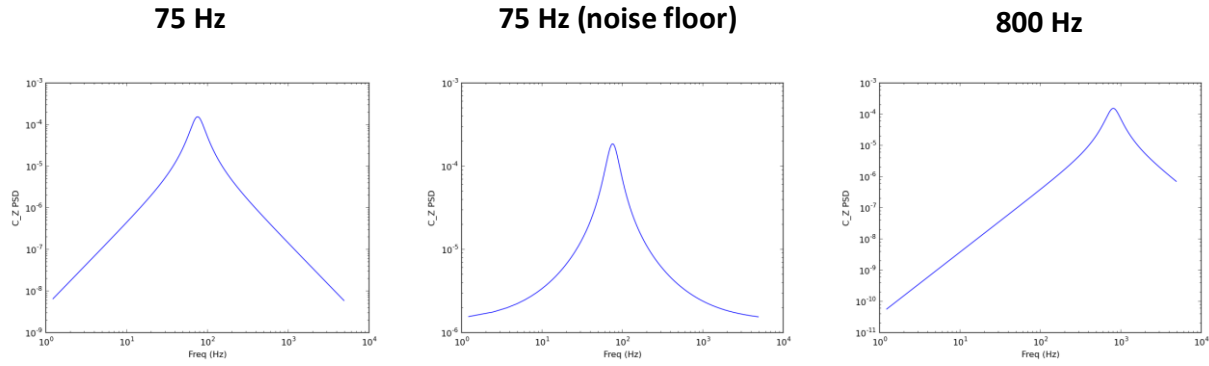


Figure 14: Parametric unsteady loading

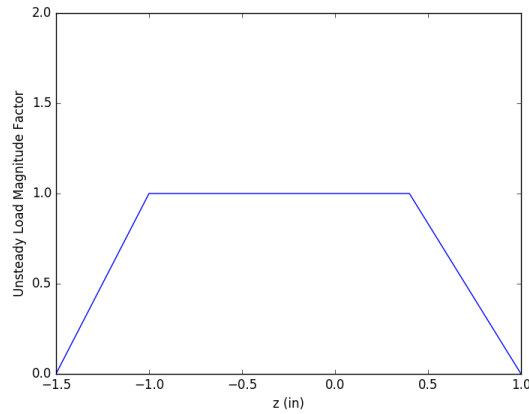


Figure 15: Position dependent magnitude scaling for parametric unsteady loading

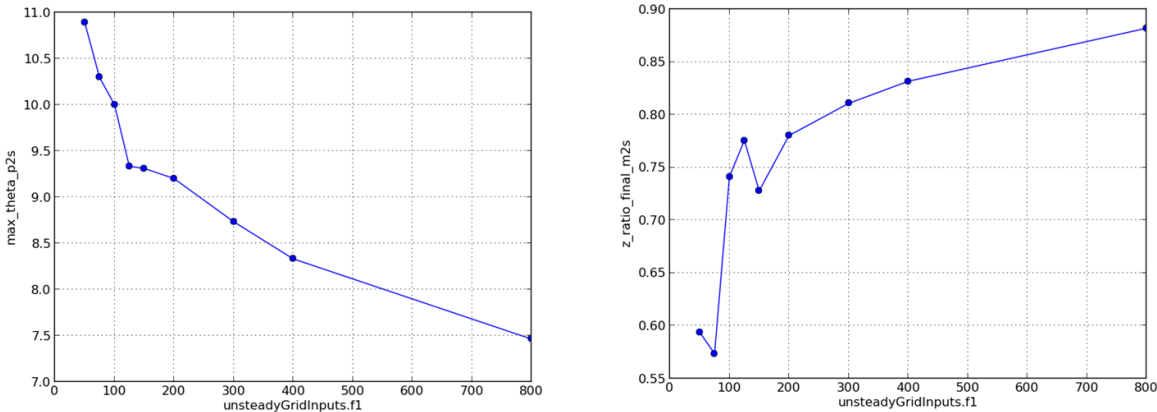


Figure 16: SSLF output metrics as a function of aeroacoustic frequency

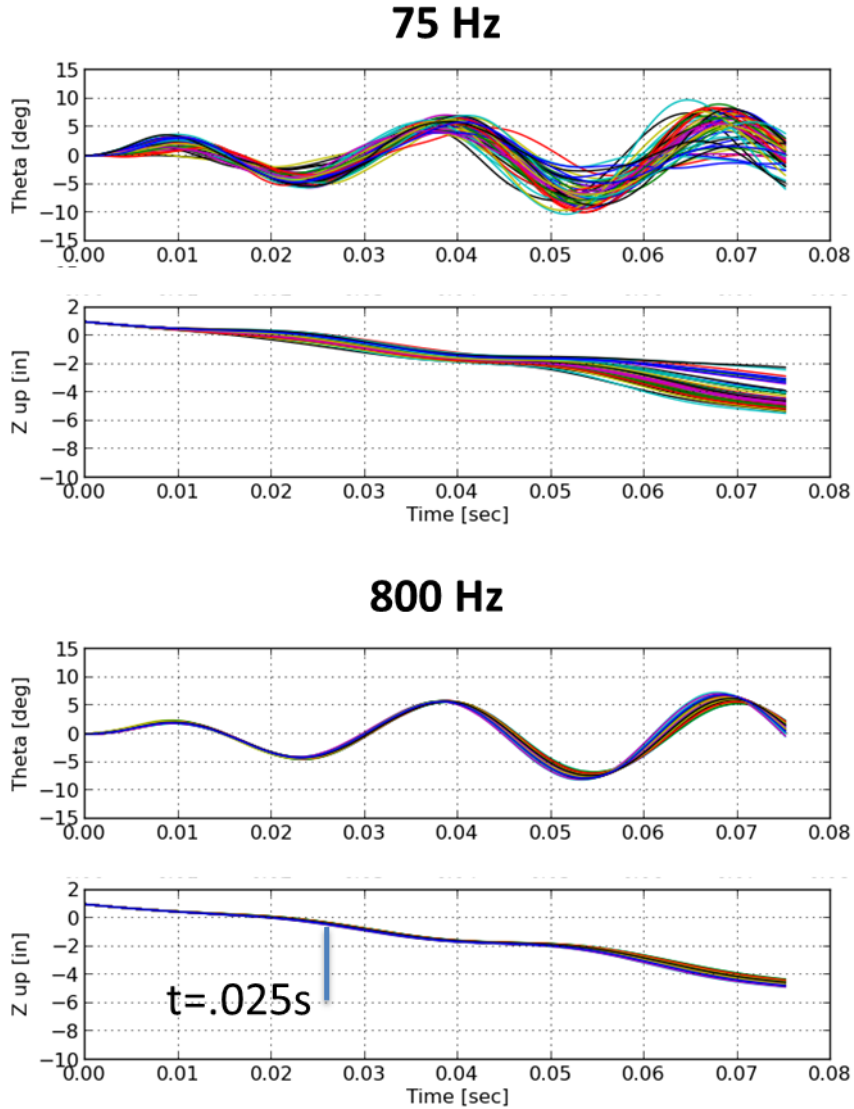


Figure 17: Multiple trajectory realizations for SSLF at high and low unsteady frequency content

IV. Conclusion

Methods for characterizing parametric relationships in store trajectories subjected to unsteady flowfields have been developed. In the case of variation in mass properties and flight condition, parametric studies can be conducted by modifying inputs to trajectory simulation while using high fidelity aerodynamic data. In the case of geometric variation, parametric study is conducted through the use of reduced fidelity models.

Parametric study on a HIFEX/GBU-38 configuration indicates that increased pitch variation is present when store CG is moved aft and when initial velocity is reduced. These trends are also present in surrogate models generated based on this simulation data.

Parametric study on flight dynamics and aeroacoustic characteristics on a generic store identifies where in the parameter space relevant frequencies coincide. As a store decreases in size, the short period frequency increases to the point that it coincides with the shear layer transit frequency. As a store further decreases in size, the short period coincides with the first Rossiter frequency on a cavity.

Parametric study of the effect of aeroacoustic frequency on trajectory for a generic store configuration indicates that the lower aeroacoustic frequencies drive an increase in trajectory variation.

Acknowledgement

Funding for this development has been provided by the Weapons Integration Team of the Air Vehicles Directorate at the Air Force Research Laboratory. The Air Force technical monitor is Ian Maatz.

References

- [1] Arnold, R. J. and Epstein, C. S. *AGARD Flight Test Techniques Series. Volume 5. Store Separation Flight Testing*. Neuilly-Sur-Seine, France : AGARD-AG-300-VOL-5, Advisory Group for Aerospace Research and Development, 1986. ADA171301.
- [2] Johnson, R., Stanek, M. and Grove , J. *Store Separation Trajectory Deviations due to Unsteady Weapons Bay Aerodynamics*. Reno : 46th AIAA Aerospace Sciences Meeting and Exhibit, 2008. AIAA-2008-188.
- [3] Roughen, K, Wang, X, Bendiksen, O, Baker, M. *A System for Simulation of Store Separation Including Unsteady Effects*. Orlando , 2009. 47th AIAA Aerospace Sciences Meeting including The New Horizons Forum and Aerospace Exposition.
- [4] Freeman, J. A. *Applied Computational Fluid Dynamics for Aircraft-Store Design, Analysis and Compatibility*. Reno : 44th AIAA Aerospace Sciences Meeting and Exhibit, 2006. AIAA 2006-456.
- [5] Murman, S. M., Aflosmis, M. J. and Berger, M. J. *Simulations of Store Separation from an F/A-18 with a Cartesian Method*. 4, Journal of Aircraft, 2004, Vol. 41.
- [6] Hosder, S., Walters, R.W., and Balch, M.,. *Point-Collocation Nonintrusive Polynomial Chaos Method for Stochastic Computational Fluid Dynamics*. 12, 2010 December, AIAA Journal, Vol. 48, pp. 2721-2730.
- [7] Russell, S., Norvig, P. *Artificial Intelligence: A Modern Approach*. Prentice Hall, 2009. ISBN 0136042597.
- [8] Robertson, G, Kumar, R, Doyle, S, Baker, M, Roughen, K, Johnson, R. *Acoustics of a Supersonic Cavity with a Generic Store*. 53rd AIAA Aerospace Sciences Meeting, 2015. AIAA 2015-1292.
- [9] Hosder, S., Walters, R., and Balch, M.,. *Efficient Sampling for Non-Intrusive Polynomial Chaos Applications with Multiple Uncertain Input Variables*. Honolulu, HI, 2007. 9th AIAA Non-Deterministic Approaches Conference. AIAA Paper 2007-1939.
- [10] Hosder, S., and Walters, R.W. *Non-Intrusive Polynomial Chaos Methods for Uncertainty Quantification in Fluid Dynamics*. Orlando, FL : AIAA, January 4 - 7, 2010. 48th AIAA Aerospace Sciences Meeting.
- [11] Winter, T. *M4 UQ Framework User's Manual*. 2013 : M4 Engineering. Version 2.0.